Chinese Chemical Letters 33 (2022) 3762–3766

Contents lists available at ScienceDirect

Chinese Chemical Letters

journal homepage: www.elsevier.com/locate/cclet

Electrochemical deposition of uranium oxide with an electrocatalytically active electrode using double potential step technique

Jie Huang[a], Zhirong Liu[a,b], Dejuan Huang[b], Tianxiang Jin[a], Yong Qian[a,b,*]

[a] Jiangxi Province Key Laboratory of Polymer Micro/Nano Manufacturing and Devices, East China University of Technology, Nanchang 330013, China
[b] State Key Laboratory of Nuclear Resources and Environment, East China University of Technology, Nanchang 330013, China

ARTICLE INFO

Article history:
Received 7 August 2021
Revised 16 September 2021
Accepted 3 November 2021
Available online 10 November 2021

Keywords:
Electrochemical deposition
Uranium
Double potential step technique
Graphene oxide
Nanocomposites

ABSTRACT

The development of effective uranium-removal techniques is of great significance to the environment and human health. In this work, a double potential step technique (DPST) was applied to remove U(VI) from uranium-containing wastewater using a carbon felt electrode modified by graphene oxide/phytic acid composite (GO-PA@CF). The application of DPST can inhibit water splitting and prevent GO-PA from adsorbing other interfering ions in wastewater. The GO-PA composite can effectively accelerate the electrochemical reduction rate of U(VI), which significantly improved the electrochemical deposition rate of uranium oxide. As a result, the maximum removal efficiency and maximum removal capacity of GO-PA@CF electrode reached 98.7% and 1149.3 mg/g, respectively. The removal efficiency remained 97.2% after five cycles of reuse. Moreover, the removal efficiency of GO-PA@CF electrode can reach more than 70% in simulated wastewater.

As a radioactive heavy metal, uranium poses a great threat towards environment and human health. With the widespread use of nuclear energy, the world's consumption of uranium resources has increased sharply [1]. As a result, a large amount of uranium-containing wastewater will be produced in uranium mine tailings. When this wastewater enters the soil, it will cause serious soil pollution and groundwater pollution. Furthermore, uranium released into the biosphere will inevitably harm human health through the food chain [2–4]. Therefore, uranium in wastewater needs to be separated and recovered efficiently.

The chemical/physical adsorption technique is one of the most common methods for uranium-containing wastewater treatment [5,6]. The removal mechanism of this method is mainly attributed to chelation and ion-exchange. The selective adsorption of uranium ion can be easily achieved by designing the adsorption active sites with specific chemical structure, such as phosphate and amidoxime group [7,8]. However, this adsorption method has several disadvantages: (1) The adsorption capacity is limited by the number of adsorption sites, which leads to a low adsorption capacity [9]; (2) the adsorption rate is usually low, since the adsorption process of the chemical/physical adsorption depends on the random diffusion rate of ions. Thus, it is not suitable for treating the wastewater containing uranium with a low concentration [10].

Capacitive deionization is another ideal method to remove uranium ions from uranium-containing wastewater [11,12]. This method refers to the adsorption of ions on the surface of electrode material by applying an electric field in the solution [13]. The diffusion rate of uranium ions can be accelerated by the electric field, which leads to a higher deposition rate compared with that of other adsorption methods. This advantage is more obvious in the treatment of uranium solution with a low concentration, for example, extracting uranium from seawater. Moreover, uranium ions can be reduced to insoluble UO_2 on the electrode surface, which makes the removal capacity much larger [14]. Nevertheless, this technique also has its own drawbacks: (1) The selectivity of capacitive deionization is poor. Wastewater from uranium mines often contains many kinds of metal ions, such as calcium, magnesium and iron. These metal ions will be deposited on the surface of electrode materials together with uranium ions, thus limiting the removal efficiency [15]. (2) The requirements for the electrode materials are rigorous. Ideal electrode materials for capacitive deionization should have excellent electrochemical inertness, high electronic conductivity and large specific surface area [11,16].

In this work, we try to integrate the superiority of both chemical adsorption and capacitive deionization above to demonstrate

* Corresponding author.
E-mail address: yqianecit@163.com (Y. Qian).

https://doi.org/10.1016/j.cclet.2021.11.008
1001-8417/

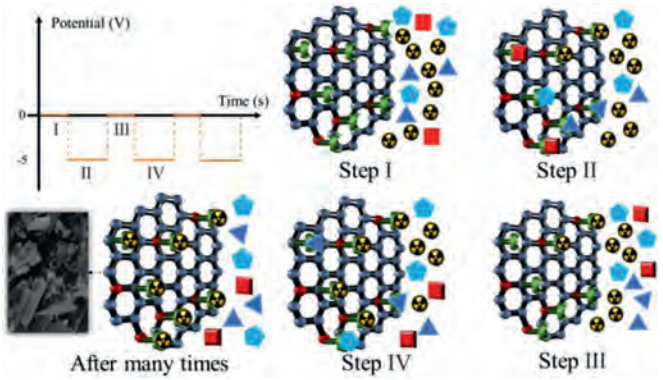

Fig. 1. Schematic of double potential step technique (DPST).

an efficient electrochemical deposition technique for radionuclide removal. Therefore, we designed a carbon felt/phytic acid modified graphene oxide composite (GO-PA@CF) as the electrode material for the electrochemical adsorption of uranium. Carbon felt (CF) not only has remarkable electrochemical and radiation inertness, but also has excellent conductivity, so it is suitable to be used as current collector [17]. Phytic acid (PA) is a nontoxic biological molecule, which contains six phosphate groups. Considering the strong binding interactions between phosphate groups and uranyl ions, it is used as the selective adsorption sites for removing uranium [18,19]. Graphene oxide has a larger specific surface area, better hydrophilicity and abundant polar functional groups compared with carbon felt [20–22]. Therefore, it is applied as a carrier of phytic acid to combine the CF and PA molecules together.

In addition to the removal mechanism and structure design, the operation mode is also an important factor affecting removal performance. In the process of electrochemical deposition, the applied direct current voltage will lead to serious water splitting [10].

Furthermore, continuous high voltage will induce a large number of competitive ions to occupy the active sites, resulting in the decline of removal efficiency [23]. To overcome this problem, a double potential step technique (DPST) was adopted for uranium extraction from uranium-containing wastewater. In this method, a voltage that alternates periodically between zero and a negative value is applied to the solution. The details of this method are shown in Fig. 1. In the initial state (step I), all ions in the solution were randomly dispersed. In step II, an electric field is applied to the solution. As a result, all cations migrate towards the GO-PA@CF electrode and interact with the phosphate groups on its surface. Meanwhile, part of the as-adsorbed uranium ions is reduced to insoluble UO_2 and then deposited on the electrode surface. In the third step, the electric field intensity becomes zero. Due to the strong interaction between uranium ion and phosphate group, uranium ions can still adhere to the surface of electrode material after the end of periodic voltage. However, other metal ions which are not firmly combined with the phosphate group will separate from the phosphate group and diffuse into the solution due to Coulomb repulsion. This effect can make a great portion of adsorption groups regain adsorption activity, which ensures the high removal efficiency of the electrode material. With the repeated application of the alternating voltage, most of the uranium ions will be reduced to UO_2, and the purpose of selective removal of uranium ions can be achieved (step IV). Moreover, the kinetic rate of uranium reduction is usually much higher than that of hydrogen evolution [10]. Therefore, the water splitting in the waste water can also be effectively restrained by raising the frequency of the periodic voltage to a proper value.

The surface morphologies of GO-PA@CF composite were investigated by scanning electron microscopy (SEM). As seen in Fig. 2, the

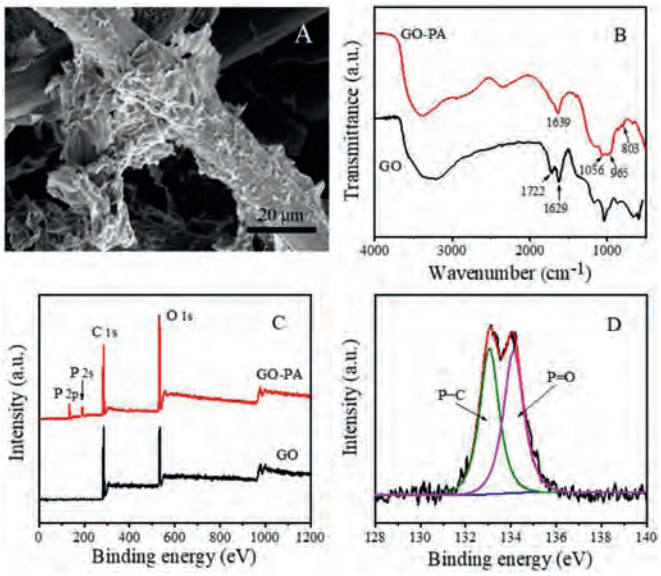

Fig. 2. (A)SEM images of GO-PA@CF. (B) FTIR spectra of the GO and GO-PA. (C) XPS spectra of the GO and GO-PA. (D) High-resolution XPS P 2p of GO-PA.

GO sheets showed wrinkled and crumpled features and it coated tightly on the smooth surface of carbon felt, which confirms that the GO were successfully adhered to carbon felt by electrodeposition. The chemical structure of GO and GO-PA was examined by FT-IR (Fig. 2). Two peaks centered at 1722 and 1629 cm^{-1} in the GO spectra were assigned to C=O carboxyl stretching vibration and C=C framework vibration, respectively [24]. Compared with the pristine GO, GO-PA showed typical peaks at 1056 and 1639 cm^{-1}, corresponding to phosphate radical and phosphate hydrogen radical, respectively. In addition, the peaks of the P−O−C bonds were observed at 965 and 803 cm^{-1} [19,25]. The X-ray photoelectron spectroscopy (XPS) analysis (Fig. 2C) showed that the new peaks of P 2p and P 2 s were observed at 134.2 and 191.1 eV in the spectrum of GO-PA, respectively. These results further confirm the successful modification of GO. The P 2p spectrum (Fig. 2D) presented two peaks at 133.2 and 134.6 eV, corresponding to P−C and P−O bonds, respectively [26,27]. The above characterization results prove that GO-PA@CF was successfully synthesized.

Electrochemical impedance spectra measurements were used to investigate the electrochemical characteristics of CF and GO-PA@CF and the Nyquist plots were shown in Fig. 3A. The intercept of the curve with X axis corresponds to the equivalent series resistances (R_s), which is the combination of the ionic resistance of electrolyte and the resistance of the electrode material [28]. The R_s (3.3 Ω) of the GO-PA@CF electrode is higher than that of the CF (2.2 Ω), which is caused by the low electron conductivity of GO coated on the surface of CF. The diameter of the semicircle in the curve corresponds to the charge transfer resistance (R_{ct}) [29]. The value of R_{ct} for CF and GO-PA@CF is 0.5 Ω and 0.6 Ω, respectively. The higher R_{ct} can still be attributed to the low electron conductivity of GO. The slope of the curve at the low frequency is related to the diffusion of ions in electrode materials [30]. The straight line in the low frequency region for CF was steeper than that for GO-PA@CF, which indicates that the diffusion of ions in electrode materials is hindered by the graphene oxide sheets.

The cyclic voltammetry scan curves of GO-PA@CF in 1 mol/L Na_2SO_4 solution at 100 mV/s with different uranyl nitrate concentrations are displayed in Fig. 3B. There was no obvious redox peak in the curve without uranyl ion, so the peaks in the scan curves of 100 mg/L and 1000 mg/L uranyl nitrate can be identified as the redox peaks of uranium. Both 100 mg/L and 1000 mg/L uranyl nitrate

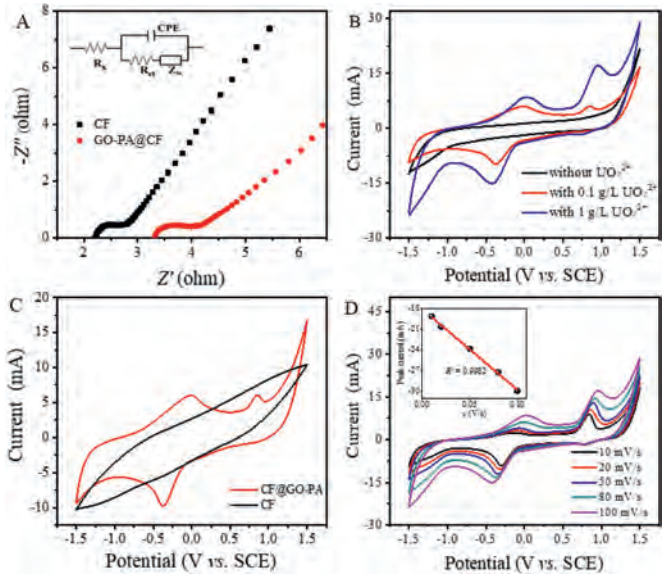

Fig. 3. (A) The electrochemical impedance spectra of CF and GO-PA@CF, the inset shows the electric equivalent circuit. (B) CV curves of the GO-PA@CF electrode in different concentrations of uranyl nitrate solution. (C) CV curves of the CF and GO-PA@CF electrodes in 100 mg/L uranyl nitrate solution. (D) CV curves of the GO-PA@CF electrode in 1000 mg/L uranyl nitrate solution at different scan rate. The inset shows the plot of peak current versus scan rate (v) for cathodic peaks.

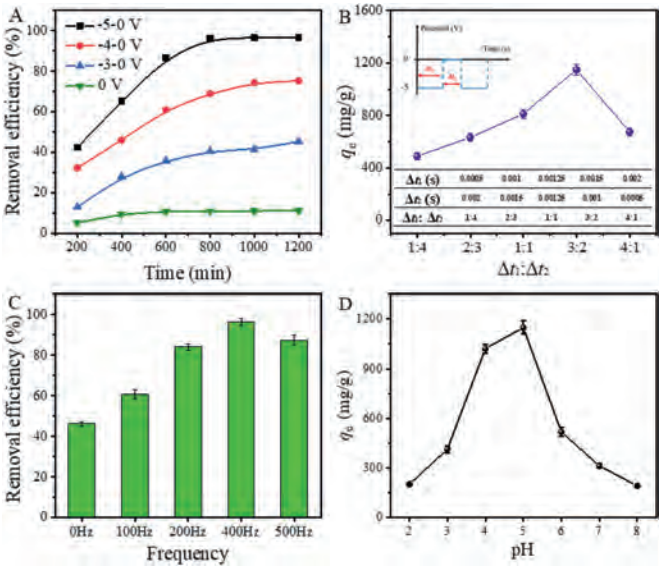

Fig. 4. (A) The removal performance of GO-PA@CF under different alternating voltages (Δt_1:Δt_2 = 3:2, 400 Hz, pH 5). (B) The removal capacities of GO-PA@CF under different power-on/off time ratios (−5 V, 400 Hz, pH 5). (C) Effect of pulse frequency on uranium sorption by GO-PA@CF (Δt_1:Δt_2 = 3:2, −5 V, pH 5). (D) Effect of initial solution pH on uranium sorption by GO-PA@CF (Δt_1:Δt_2 = 3:2, −5 V, 400 Hz). All experiments were conducted in an aqueous solution of uranyl nitrate with a concentration of 100 mg/L.

solutions exhibited a reduction peak around −0.3 V, corresponding to the one-electron reduction of from U(VI) to U(V). The oxidation peak at 0.1 V is caused by the oxidation from U(V) to U(VI) [31,32]. Notably, the reduction peak of U(VI) is evidently bigger than the oxidation peak of U(V). That is because UO_2^+ is unstable, and it tends to disproportionate into UO_2^{2+} and UO_2 spontaneously. UO_2 is difficult to dissolve in aqueous solution, and it will be deposited on the electrode surface in a solid state and eventually removed from the solution. The CV curves of the CF and GO-PA@CF electrodes in 100 mg/L uranyl solution were shown in Fig. 3C. The redox peak of uranium ion can hardly be observed in the curve of CF electrode, but it can be observed in the curve of GO-PA@CF electrode. This phenomenon indicates the fact that although GO-PA@CF has a lower conductivity and ion diffusion rate than that of CF, it can accelerate the redox reaction more effectively.

In order to further study the electrochemical catalytic mechanism of GO-PA material, the effect of the scan rates on the cyclic voltammograms of GO-PA@CF electrode with 1000 mg/L uranyl nitrate solution was investigated. As seen from Fig. 3D, the redox peak area of uranium ions increased significantly with the increase of scan rate. It is known that the peak current is proportional to the scan rate for adsorption-controlled electrochemical reaction, and the peak current is proportional to the square root of scan rate for diffusion-controlled reaction [31]. The inset of Fig. 3D displayed the linear relationship between the peak values of reduction current and the scan rates (R^2 = 0.998). Therefore, it can be confirmed that the electrochemical reduction of uranium ions in the presence of GO-PA is governed by adsorption-controlled mechanism: The uranium ion in solution is adsorbed on GO-PA surface before being electrochemically reduced, resulting in a lower electro-reduction barrier caused by the combination of uranium ion and phosphate group.

Experimental parameters, including voltage, power-on/off time ratio, pulse frequency and solution pH, were investigated to determine the optimal operating conditions of the GO-PA@CF electrode. The effect of voltage on the electrochemical deposition property of GO-PA@CF was investigated and the results were shown in Fig. 4A. The removal efficiency of GO-PA@CF under no voltage condition was about 15%, which was much lower than that of GO-PA@CF electrode under the alternating voltage. This result manifests that the chemical adsorption of GO-PA cannot effectively remove uranium ions due to the limitation of the number of adsorbed functional groups. With the increase of voltage, the removal efficiency of GO-PA@CF electrode increases gradually. The best removal performance can be obtained under the alternating voltage of −5 V, and the maximum removal efficiency is 98.7%

The effect of power-on/off time ratio on the removal capacity was exhibited in Fig. 4B. The removal capacity of GO-PA@CF reached the maximum value when the power-on/off time ratio was 3:2. The values of power-on time (Δt_1) and power-off time (Δt_2) under different time ratios are listed in the inset of Fig. 4B. When the time ratio was less than 3:2, the contact time between uranyl ion and GO-PA is short, resulting in a large number of adsorption active groups on GO-PA unable to effectively chelate with uranyl ions. When the time ratio was higher than 3:2, the power-on time is relatively long, which may accelerate the hydrolysis reaction, and thus limit the electrochemical deposition performance of the GO-PA@CF electrode [10]. The effect of pulse frequency on the removal efficiency was shown in Fig. 4C. When the frequency was lower than 400 Hz, the removal efficiency of GO-PA decreased significantly with the decrease of frequency. This is because a longer power-on time is more conducive to the electrolysis of water molecules and weakens the electrochemical reduction efficiency [10]. Fig. 4D showed the effect of initial solution pH on uranium extraction by GO-PA@CF. This experiment was carried out under an alternating voltage of −5 V, and the power-on/off time ratio was 3:2. The maximum removal capacity was 1149.3 mg/g at pH 5. When the pH value was less than 5, the rate of the hydrogen evolution reaction increased, which interfered with the electrochemical reduction of uranium [33]. When the pH was higher than 5, UO_2^{2+} will be hydrolyzed to form the complexes of $(UO_2)_2(OH)_2^{2+}$, $(UO_2)^3(OH)^{5+}$ and $(UO_2)_4(OH)^{7+}$, which may weaken the interaction between uranium ions and GO-PA@CF [34]. Fig. S1 (Supporting information) is the simulation result for the existing form of U(VI) in aqueous solution at different pH. It

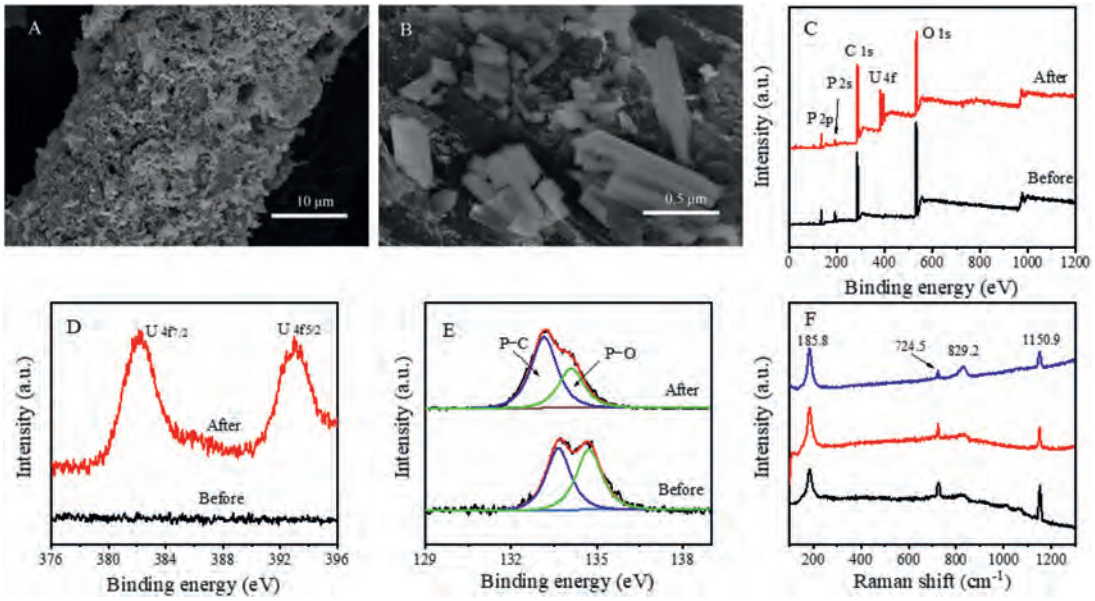

Fig. 5. (A) SEM image of the GO-PA@CF electrode after 14 h electrochemical deposition. (B) High-Magnification SEM image of GO-PA@CF electrode. (C) XPS spectra of GO-PA@CF before and after extraction. (D) High-resolution XPS U 4f of GO-PA@CF before and after extraction. (E) High-resolution XPS P 2p of GO-PA@CF before and after extraction. (F) The Raman spectra of the electrochemically deposited particles.

Table 1
The extraction performances of the GO-PA@CF electrode at different initial concentrations.

Concentrations of U(VI) (mg/L)	10	20	50	100
Removal capacity (mg/g)	274.12	441.26	636.78	1149.26
Removal efficiency (%)	98.68	97.08	96.79	96.54

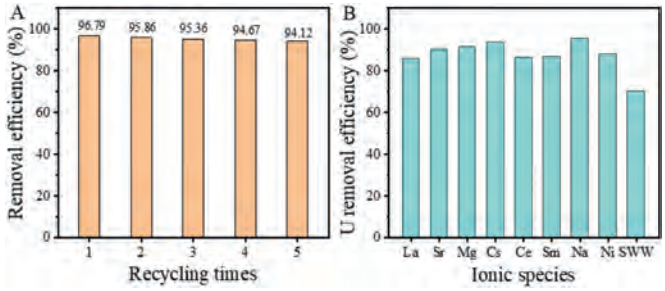

Fig. 6. (A) The repeatability of the GO-PA@CF electrode for uranium extraction. (B) The removal efficiency of GO-PA@CF towards uranium in the present of different interfering ions.

can be seen that the form of uranium present in water depends strongly on the pH. When the pH was less than 5, uranium is mainly present as UO_2^{2+}. As the pH increases, U(VI) is hydrolyzed and transformed gradually to anion. This simulation result can well support the previous results.

The extraction performances of the GO-PA@CF electrode at different initial concentrations of U(VI) were evaluated, and the results were shown in Fig. S2 (Supporting information) and Table 1. It can be seen that GO-PA@CF can maintain its removal efficiency above 96% in all four cases. Furthermore, its removal capacity increased evidently as the initial concentration increased, and reached the maximum value (1149.3 mg/L) when the concentration is 100 mg/L. The excellent extraction performance of GO-PA@CF can be attributed to the following two points: (1) The DPST technique and the corresponding experimental parameters adopted in this work ensure that the electrochemical deposition system can work at a relatively low voltage without evident water splitting, which greatly improves the removal efficiency of uranium ions. (2) The excellent electrochemical catalytic performance of GO-PA can accelerate the reduction of uranium ions, and rapidly reduces the adsorbed uranyl ions to uranium oxide. Subsequently, the uranium oxide precipitates from the solution and releases the active functional groups simultaneously.

The morphology of the GO-PA@CF electrode after the DPST extraction experiment was investigated by SEM. As shown in Fig. 5A, a large number of particles are attached to the electrode surface. Higher magnification of the SEM image (Fig. 5B) showed that these particles are irregular prism with a size of about 0.5 μm.

The XPS measurement was applied to study the chemical structure of GO-PA@CF electrode after the DPST extraction experiment. Two sharp peaks at 392.9 and 382.2 eV in XPS spectra correspond to U $4f_{5/2}$ and U $4f_{7/2}$, respectively, indicating that the uranyl species were successfully attached on the surface of GO-PA@CF electrode (Figs. 5C and D). The P 2p high-resolution XPS spectrum before and after extraction was shown in Fig. 5E. The intensity of P—O peak decreased markedly, and the binding energy of P—O shifted from 134.7 eV to 134.1 eV after electrochemical deposition, suggesting that the P—O groups may be involved in the complexation with uranium oxide [35].

Raman spectroscopy was used to further determine the chemical structure of the electrochemically deposited particles on the surface of GO-PA@CF electrode. To ensure the accuracy of the experimental results, the samples at three different regions were measured. As shown in Fig. 5F, the Raman spectra of the three samples were almost the same, indicating that the sample surface has a uniform chemical structure. The bands at 185.8, 724.5 and 829.2 cm^{-1} are the characteristic bands of U_3O_8, and the band at 1150.9 cm^{-1} is the characteristic bands of UO_2 [36,37]. These results indicate that the particle deposited on the electrode is a mixture of U_3O_8 and UO_2.

The reusability of GO-PA@CF was investigated in 50 mg/L uranyl nitrate solution (Fig. 6A). The uranium oxide particles on the electrode were eluted in 0.1 mol/L HCl solution assisted by a reverse

periodic voltage (0–5 V, 400 Hz, $\Delta t_1:\Delta t_2 = 3:2$). The elution process lasted for 10 h. After five cycles of reuse, the removal efficiency of GO-PA@CF remained 97.2%. This result indicated that GO-PA@CF has an excellent reusability, which can be attributed to its excellent electrochemical stability and radiation inertness.

Interference experiments were conducted to investigate the selectivity of GO-PA@CF towards uranium in simulated wastewater (SWW). The SWW contained La^{3+}, Sr^{2+}, Mg^{2+}, Cs^{+}, Ce^{3+}, Sm^{3+}, Na^{+}, and Ni^{2+}. All concentrations of the solutes used in these experiments were 50 mg/L. Moreover, the removal efficiencies in the present of single interfering ions in SWW were also measured separately.

As shown in Fig. 6B, the removal efficiencies of GO-PA@CF can reach more than 85.7% in the presence of different single interfering ions. Even in SWW, the removal efficiency can be maintained at about 70%. This excellent selectivity is mainly attributed to the alternating nature of the voltage. When voltage is applied, uranium ions and coexisting ions are firmly combined with phosphate groups on the electrode surface due to the action of electric field. However, compared with other coexisting ions, uranium ions have stronger interactions with phosphate groups. Therefore, after the voltage is removed, the coexisting ions will separate from the electrode surface due to the Coulomb repulsion, while uranium ions will still be adsorbed on the electrode surface. Therefore, this method can effectively eliminate the interference of coexisting ions.

In this work, the GO-PA@CF electrode for removing uranium ions from uranium-containing wastewater is prepared by a simple ultrasonic and electrodeposition method. A double potential step technique (DPST) was used to inhibit water splitting and prevent GO-PA from adsorbing other interfering ions in wastewater. The excellent electrochemical catalysis of GO-PA can accelerate the electrochemical reduction of uranium ions, which further improves the removal efficiency of uranium ions. Furthermore, we comprehensively studied the effect of experimental operating parameters on the removal efficiency of GO-PA@CF electrode. It is found that GO-PA@CF has the best uranium removal performance when the power-on/off time ratio is 3:2, pulse frequency is 400 Hz, the pH value of the solution is 5, and the alternating voltages is −5 V. Under the above optimum experimental conditions, the removal capacity of the GO-PA@CF electrode can reach 1149.3 mg/g and the maximum removal efficiency can reach 98.7%. Moreover, the removal system also has a good repeatability and a high selectivity for U(VI) extraction from simulated wastewater.

Declaration of competing interest

The authors declare no conflict of interest.

Acknowledgment

The authors are grateful for the financial support of the National Natural Science Foundation of China (Nos. 41361088 and 41867063).

Supplementary materials

Supplementary material associated with this article can be found, in the online version, at doi:10.1016/j.cclet.2021.11.008.

References

[1] J.A. Kazery, G. Proctor, S.L. Larson, et al., ACS Earth Space Chem. 5 (2021) 356–364.
[2] P. Kumari, G. Kumar, S. Prasher, et al., Environ. Earth Sci. 80 (2021) 271.
[3] S. Shi, X. Tang, Y. Yang, Z. Liu, J. Radioanal. Nucl. Chem. 328 (2021) 507–517.
[4] M.L.B.d. Moraes, A.C.Q. Ladeira, Chemosphere 277 (2021) 130131.
[5] Y. Shen, N. Chu, S. Yang, et al., Ind. Eng. Chem. Res. 58 (2019) 18329–18335.
[6] D.C. Wang, Y.H. Li, D. Li, Y.Z. Xia, J.P. Zhang, Renew. Sustain. Energy Rev. 14 (2010) 344–353.
[7] N. Tang, J. Liang, C. Niu, et al., J. Mater. Chem. A 8 (2020) 7588–7625.
[8] L. Li, R. Ma, T. Wen, et al., Sci. Total Environ. 694 (2019) 133697.
[9] C. Liu, T. Wu, P.C. Hsu, et al., ACS Nano 13 (2019) 6431–6437.
[10] C. Liu, P.C. Hsu, J. Xie, et al., Nat. Energy 2 (2017) 17007.
[11] L. Chen, D.G. Tong, Sep. Purif. Technol. 250 (2020) 117175.
[12] Y. Oren, Desalination 228 (2008) 10–29.
[13] W. Wang, S. Liu, Y. Zhou, et al., Sep. Purif. Technol. 276 (2021) 119235.
[14] J. Zhou, H. Zhou, Y. Zhang, et al., Chem. Eng. J. 398 (2020) 125460.
[15] J. Gamaethiralalage, K. Singh, S. Sahin, et al., Energy Environ. Sci. 14 (2021) 1095–1120.
[16] H. Liu, J. Zhang, X. Xu, Q. Wang, Chem. Eur. J. 26 (2020) 4403–4409.
[17] P. Xue, S. Jiang, W. Li, et al., Bioprocess Biosyst. Eng. 44 (2021) 1119–1130.
[18] D. Yuan, S. Zhang, J. Tan, et al., Sep. Purif. Technol. 237 (2020) 116379.
[19] D. Wang, F. Xu, J. Hu, M. Lin, Mater. Sci. Eng. C 71 (2017) 1086–1089.
[20] S. Liu, C. Luo, L. Chai, J. Ren, J. Solid State Electrochem. 25 (2021) 1975–1985.
[21] Z.Y. Han, L.J. Huang, H.J. Qu, et al., J. Mater. Sci. 56 (2021) 9545–9574.
[22] M. Pumera, Electrochem. Commun. 36 (2013) 14–18.
[23] W. Wang, J. Luo, W. Wei, et al., Chemosphere 271 (2021) 129531.
[24] A.V. Ramya, N. Joseph, M. Balachandran, Nanobiotechnol. Rep. 16 (2021) 183–187.
[25] H. Nan, L. Zhu, H. Liu, W. Li, Appl. Surf. Sci. 355 (2015) 1215–1221.
[26] Z. Zhang, Z. Dong, X. Wang, et al., Chem. Eng. J. 370 (2019) 1376–1387.
[27] A.M. Puziy, O.I. Poddubnaya, R.P. Socha, J. Gurgul, M. Wisniewski, Carbon 46 (2008) 2113–2123.
[28] T. Jin, J. Chen, C. Wang, Y. Qian, L. Lu, J. Mater. Sci. 55 (2020) 12103–12113.
[29] K. Narthana, G. Durai, P. Kuppusami, et al., Int. J. Energy Res. 45 (2021) 9983–9998.
[30] J. Chen, C. Lin, M. Zhang, T. Jin, Y. Qian, Chem. Electro. Chem. 7 (2020) 3311–3318.
[31] S.K. Guin, A.S. Ambolikar, J.V. Kamat, RSC Adv. 5 (2015) 59437–59446.
[32] Y. Peled, E. Krent, N. Tal, H. Tobias, D. Mandler, Anal. Chem. 87 (2015) 768–776.
[33] E.J. Kelly, H.R. Bronstein, J. Electrochem. Soc. 131 (1984) 2232–2238.
[34] J. Xiao, Y. Jing, Y. Yao, X. Wang, Y. Jia, J. Mol. Liq. 277 (2019) 843–855.
[35] S. Mishra, J. Dwivedi, A. Kumar, N. Sankararamakrishnan, New J. Chem. 40 (2016) 1213–1221.
[36] C. Jégou, R. Caraballo, S. Peuget, et al., J. Nucl. Mater. 405 (2010) 235–243.
[37] D. Manara, B. Renker, J. Nucl. Mater. 321 (2003) 233–237.